 FDMP, vol.13, no.1, pp.19-36, 2017

Investigation of the Melting Coupled Natural Convection of Nano Phase Change Material: A Fan Less Cooling of Heat Sources

Mustapha FARAJI[1]

Abstract: A two-dimensional numerical model that accounts for heat transfer by conduction and natural convection in the molten region of nano enhanced Phase Change Material (PCM) is performed. Numerical investigations were conducted using an enthalpy-porosity method in order to examine the impact of the dispersion of copper (CuO) nanoparticles on the heat source temperature and the effect on the heat sink secured working time and the melting rate. Results show that heat spreads more easily along the conducting plate and to the PCM and, consequently, the PCM melts rapidly and the heat source is efficiency cooled by the addition of nanoparticles. In contrast, the heat source secured working time decreases for high nanoparticles fraction.

Keywords: Nanoparticles, PCM, melting, latent heat storage, thermal control, natural convection, heat source.

Nomenclature

c_p	specific heat, J kg^{-1} K^{-1}
d_p	nanoparticle diameter, m
e_c	heat source thickness, m
e_s	substrate (plate) thickness, m
F	liquid fraction
h	enthalpy, J kg^{-1}
H_m	height of the enclosure, m
K	thermal conductivity, W m^{-1} K^{-1}
L_c	heat source length, m
L_m	width of the enclosure, m
P	pressure, Pa
Q'	heat generation per unit length, W m^{-1}

[1] Laboratory of Physics of Materials, Microelectronics, Automatics and Thermal Sciences, LPMMAT, Physics Department, Faculty of Sciences Ain Chock, Hassan II University, Casablanca-Morocco.
Email: farajimustapha@yahoo.fr.

S	source term
t	time, s
T	temperature, °C
u, v	x, y velocity, m s^{-1}

Subscripts

c	heat sources
Cr	critical value
L	liquid, local
m	melt, PCM
Max	maximum value
Nf	Nanofluid
P	Nanoparticle
ref	reference value
S	wall, solid

Greek symbols

ΔH_f	latent heat, J kg^{-1}
β	volumetric thermal expansion factor of liquid, K^{-1}
$\delta_{1,2}$	chronicler symbols
η	perpendicular to the solid wall
ρ	density, kg m^{-3}
μ	dynamics viscosity, kg m^{-1} s^{-1}
ν	kinematic viscosity, m^2 s^{-1}

1 Introduction

Phase Change Materials (PCMs) are used to absorb and release thermal energy during transient heating and cooling. PCMs have been used successfully at large scales for solar energy storage, in energy efficient building materials [Castellón and Nogués (2007)], and at small scales in cooling portable electronics [Faraji and El Qarnia (2009)]. However, the low thermal conductivity of most PCMs results in poor heat removal. Indeed, during phase change process, the melting front moves away from the heat transfer surface. The surface heat flux decreases with respect to time, due to the increasing thermal resistance of the growing layer of molten medium, as the thermal conductivity of the ordinary PCM is low. To overcome this problem, a wide range of investigations were carried out aiming to enhance the apparent thermal conductivity of the PCM and increase the heat transfer performance. These techniques typically involve geometry optimizations of PCM based heat sinks [Tong, Khan and Amin (1996); Gong, Devahastin and Mujumdar (1999); Saha, Srinivasan and Dutta (2008)] and embedding a matrix material of high thermal conductivity within the PCM. These techniques improve the thermal response the PCM heat sink, but can displace a significant amount of PCM, reducing the total energy storage

capacity and increase the weight of the module.

A further important contribution to the cooling issue may be derived by the replacement of traditional heat transfer fluids with nanofluids. These are a new type of heat transfer fluids consisting of suspensions of nanoparticles, whose effective thermal conductivity has been demonstrated to be higher than that of the corresponding pure base liquid [Bianco, Manca, Nardini et al. (2015)]. Eastman, Choi, Thompson et al. (1997) showed that an increase in thermal conductivity of approximately 60% can be obtained for a nanofluid consisting of water and 5% Cu nanoparticles. This is attributed to the increase in surface area due to the suspension of nanoparticles. Afrouzi and Farhadi (2013) investigated mixed convection in a cavity filled with nanofluid using a cubical heater located inside the cavity in different positions. They found an enhancement in heat transfer with the increase of nanoparticle volume fraction. Metallic nanoparticles are desirable candidates for PCM enhancement without significant displacement. Bouchoucha and Bessaih (2015) investigated numerically the natural convection in a square cavity filled with a nanofluid. The left and right vertical walls of the cavity are maintained at hot and cold temperature. Horizontal walls are assumed to be adiabatic. They found that the velocity magnitude increases according to the copper nanoparticle fraction increasing. Wu, Zhu, Zhang et al. (2010) studied the potential of Al_2O_3-H_2O nanofluids as a new phase change material for the cold storage of cooling systems. The thermal response test shows that the addition of nanoparticles remarkably decreases the supercooling degree of water, advances the beginning freezing time and reduces the total freezing time. They showed that by adding 0.2% Al_2O_3 nanoparticles, the total freezing time of Al_2O_3-H_2O nanofluids can be reduced to 20.5%.

Hao and Tao (2004) studied the simulation of the laminar hydrodynamic and heat transfer characteristics of suspension flow with nano PCM particles in a microchannel. Khodadadi and Hosseinizadeh (2007) reported a numerical solution on improvement of thermal storage energy using nanoparticle enhanced phase change material. They found that the resulting nanoparticle enhanced phase change materials exhibit enhanced thermal conductivity in comparison to the base material. In addition, their numerical results showed reduction in the overall solidification time. The melting of paraffin wax dispersed with Al_2O_3 nanoparticles that is heated, at constant temperature, from one side of a square enclosure with dimensions of 25 mm x 25 mm is investigated numerically by Arasu, Arun and Mujumdar (2012). The stream function, isotherms and liquid–solid interface at different stages of the melting process are presented and discussed. The authors concluded that higher nanoparticles fractions significantly degrading natural-convection heat transfer efficacy across the melted region and the effective thermal conductivity and the latent heat storage medium can be significantly increased by using smaller volumetric concentration of alumina nanoparticles in paraffin wax.

Only few experimental works have been executed on natural convection of nanoparticle suspensions in enclosed spaces. Weinstein, Kopec, Fleischer et al. (2008) investigated the use of suspended graphite nano fibres to improve the transient thermal response of paraffin PCM embedded graphite nano-fibres. They examined the thermal effects of graphite fibre fraction 5% and graphite fibre type during the melting process for system with power loads between 3 W and 7 W. The thermal conductivity of PCMs shown a

large enhancement. They found that even at low nano fiber fraction, the nano fiber PCM mixtures were able to more effectively conduct heat and delay steady state, but an important portion of the PCM did not fully utilized. Also, Sanusi, Warzoha and Fleischer (2011) experimentally examine the effect of graphite nanofibers PCM which is embedded between two sets of aluminium fins on the thermal storage and solidification time. It found that for aspect ratios of 1, the nanographite particles shortens solidification time by as much as 61% over the base paraffin PCM. The previous cited studies used paraffin wax as the phase change material.

One of the primary disadvantages of paraffin is its low thermal diffusivity. In systems that require high heat flux removal, the poor thermal diffusivity of paraffin can lead to rapid overheat of the generating heat source. The boundary conditions reported in pervious studies are limited to isothermal boundaries or to isothermal flush mounted heat sources. For nanofluids differentially heated within square enclosures, effective thermal conductivity and dynamic viscosity are calculated, often, using traditional mean-field equations, which, originally developed for composites and mixtures with micro sized or mill sized inclusions, tend to fail in describing the thermo mechanical behaviour of nanofluids and show contradictory results.

The present study simulates the melting of Nano enhanced CuO PCM, heated from bellow by none isothermal, transient and volumetric heat source. The heat source is protruding mounted on a conducting none isothermal plate and fan less cooled by natural convection heat transfer coupled with the melting of nano PCM. The Brownian motion is taken into account to estimate the thermal conductivity of the mixture. The cooling capability of nano PCM, isotherms and dynamic field dependency on nanoparticles fraction are analysed. Also, correlations are developed for secured working time and maximum heat source temperature. The results will provide valuable insight into the potential application of nano enhanced phase change thermal management systems with higher power transient devices.

2 Mathematical modelling

Figure 1 presents the physical model. It consists of a horizontal rectangular enclosure containing a copper nano enhanced PCM (CuO, n-eicosane, T_m=47°C), heated with protruding heat source attached to the conducting plate (bottom wall).

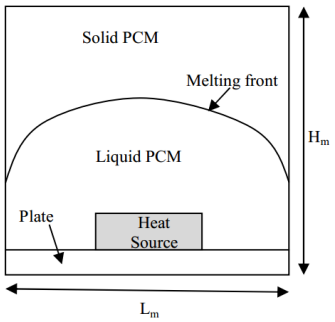

Figure 1: The physical model

The height and thickness of heat source are L_c=3 cm and e_c=0.5 cm, respectively. The height and width of the enclosure are, H_m=10 cm, and, L_m=10 cm, respectively. The thickness of the conducting plate is, e_s=0.5 cm. Heat source generates heat at constant and uniform rate, Q'=80 W/m, and dissipates that heat through their exposed faces and along the conducting plate to PCM. All enclosure boundaries are adiabatic. The bottom wall, considered as a rectangular fin, spreads and diffuses the heat to the nano PCM. Nano PCM including nanoparticles and base fluid as continuous media is Newtonian, incompressible, and assumed to be in thermal equilibrium as well as no slip condition is imposed between them.

The momentum field is subjected to no-slip boundary conditions at the solid walls. The flow is assumed two-dimensional, laminar. Effective thermal conductivity is subject to Brownian motion and depends on particle size, particle volume fraction and temperature as well as thermal properties of the base PCM. The thermo physical properties of the materials, except thermal conductivity, are constant at the temperature range under study. The density difference between solid and liquid phases of PCM is negligible, and the Boussinesq approximation is used in the momentum equation for the vertical direction. The phase change is isothermal and the PCM is initially solid at its melting temperature: $T_o = T_{ref} = T_m$

2.1 Governing equations

The general equation governing heat and mass transfer and flow in the studied configuration is:

$$\frac{\partial(\rho\Omega)}{\partial t}+\frac{\partial(\rho u\Omega)}{\partial x}+\frac{\partial(\rho v\Omega)}{\partial y}=\frac{\partial^2(\Gamma\Omega)}{\partial x^2}+\frac{\partial^2(\Gamma\Omega)}{\partial y^2}+S_\Omega \tag{1}$$

Terms of Eq. (1) are summarized in the Table 1.

Table 1: Terms of the general equation

Ω	Γ	S_Ω
1	0	0
u	μ	$-\frac{\partial p}{\partial x}+S_u$
v	μ	$-\frac{\partial p}{\partial y}+S_v$
H	k/c_p	S_T

here,
$$\begin{cases} H = \int_{T_m}^{T} c_p dT + h(T_m) \\ S_u = -C \dfrac{(1-f)?}{(f^3+b)} u \\ S_v = -C \dfrac{(1-f)?}{(f^3+b)} v + (\rho\beta)_{nf} g(T - T_m) \\ S_T = \delta_1 \left(-(1-\delta_2)\rho_{nf} \Delta H_f \dfrac{\partial f}{\partial t} + \delta_2 \dfrac{Q'}{e_c L_c} \right) \end{cases} \tag{2}$$

S_u and S_v are source terms used for the velocity suppression in the solid regions (solid PCM, plate and heat source). One of the common methods for the velocity suppression is to introduce a Darcy-like term [Voller, Cross and Markatos (1987)] (C =10^{25} kg m^{-3}s^{-1} and b=0.005 are used). The same full set of governing equations throughout the entire enclosure governs conjugate heat transfer in both the liquid and solid regions with taking a large value of the viscosity in solid regions. The conductivity k and the step function δ are expected as follows:

$$\delta_1 = \begin{cases} 1 & heat\ source, PCM \\ 0 & plate \end{cases}, \quad \delta_2 = \begin{cases} 1 & heat\ source \\ 0 & PCM \end{cases} \tag{3}$$

$$k = \begin{cases} k_{eff} & PCM \\ k_s & plate \\ k_c & heat\ source \end{cases} \tag{4}$$

The effective thermal conductivity of the nanofluid for spherical nanoparticles, subject to Brownian motion, according to Maxwell (1904) is:

$$k_{eff} = \frac{k_p + 2k_m - 2\Phi(k_m - k_p)}{k_p + 2k_m + \Phi(k_m - k_p)} k_m + 5\times 10^4 \beta\xi\phi\rho_m c_{p,m} \sqrt{\frac{BT}{\rho_p d_p}} f(T,\phi) \tag{5}$$

where B is Boltzmann constant 1.381x10^{-23} J/K, and

$$\begin{cases} \beta = 8.4407(100\phi)^{-1.07304} \\ f(T,\phi) = (2.8217\times 10^{-2}\phi + 3.917\times 10^{-3}) \dfrac{T}{T_m} + \\ \qquad (-3.0669\times 10^{-2}\phi - 3.91123\times 10^{-3}) \end{cases} \tag{6}$$

The second part of Eq. (5) accounts for Brownian motion, which causes the temperature dependence of the effective thermal conductivity. Note that there is a correction factor, ξ in the Brownian motion term, since there should be no Brownian motion in the solid phase. Its value is defined as the same as for liquid fraction, *f* in Eq. (13).

The dynamic viscosity of the nanofluid, for small particles fraction, Φ, given by Einstein (1902):

$$\mu_{nf} = (1+2.5\Phi)\,\mu_m \tag{7}$$

Different thermo physical properties of materials are expressed as follows:

$$\begin{aligned}
&(\rho\beta)_{nf} = \Phi\,(\rho\beta)_p + (1-\Phi)\,(\rho\beta)_m \ , \\
&(\rho c_p)_{nf} = \Phi\,(\rho c_p)_p + (1-\Phi)\,(\rho c_p)_m \ , \\
&\rho_{nf} = \Phi\,\rho_p + (1-\Phi)\,\rho_m \ , \ k_i = \frac{k_+ k_- (\delta_+ + \delta_-)}{k_+\delta_- + k_-\delta_+}
\end{aligned} \tag{8}$$

δ_+ and δ_- are distances separating the interface to the first neighbouring nodes, '+' and '-'. k_+ and k_- are the thermal conductivities at nodes '+' and '-', respectively.

2.2 Boundary conditions

At the interfaces between two different materials (1) and (2) (plate, PCM or heat source):

$$k_1 \left.\frac{\partial T}{\partial \eta}\right|_{interface} = k_2 \left.\frac{\partial T}{\partial \eta}\right|_{interface} \ , \ T_1 = T_2 \tag{9}$$

$$(\eta \perp \text{ interface})$$

At the adiabatic walls:

$$\left.\frac{\partial T}{\partial \eta}\right|_{wall} = 0 \tag{10}$$

No slip and non permeability at the solid interfaces and walls:

$$u=v=0 \tag{11}$$

2.3 Initial conditions

$$u=v=f=0, \ T = T_m \tag{12}$$

The governing equations are discretized using a finite volume method [Patankar (1980)].

The local liquid fraction *f* is determined iteratively from the solution of the enthalpy equation as:

$$\begin{cases} f = 1 & if \;\; T > T_m \\ f = 0 & if \;\; T < T_m \\ 0 < f < 1 & if \;\; T = T_m \end{cases} \tag{13}$$

2.4 Numerical procedure

The discretized equations are obtained by integrating the governing equations in a staggered mesh, with M and N nodes, using a control volume method developed by Patankar (1980). The power law scheme is used for the evaluation of the total flux which combines convective and conductive terms. The SIMPLE routine is used to couple pressure and velocity equations. The energy equation for PCM is solved using the enthalpy method developed by Voller (1987). The source term, $S_T = -\rho_{nf} \Delta H_f \frac{\partial f}{\partial t}$ is the central feature of this technique for the energy equation, *h*, which keeps track of latent heat evolution, and its driving element is the local liquid fraction, *f*. This fraction takes the values of 1 in fully liquid regions, 0, in fully solid regions, and lies in the interval [0, 1] in the vicinity of the melting front. In the numerical implementation, its value is determined iteratively from the solution of the energy equation. A tri-diagonal matrix iterative method is used to solve for *u*, v and *h* variables. The iterative solution continues until convergence of the flow and energy fields at every time step, is reached. Convergence is declared when the criterions relating to mass and energy balances are smaller than 10^{-7} and 10^{-3}, respectively.

2.5 Grid independence study

Numerical investigations were conducted to check the grid size and time step dependence results. The effects grid size and time step on the sensitivity of the results are shown in Table 1. Table 1a shows the effects of four grid sizes MxN: 80x80, 100x100, 120x120 and 140x140, for a time step, *dt*=0.1 s. As it can be seen, changing grid size for 120x120 to 140x140 leads to a relative change of liquid fraction and maximum temperature of 0.41% and 0.17%, respectively. Table 1b shows that using a time step of *dt*=0.1 s and 0.05s leads to relative changes of liquid fraction and maximum temperature of 0.83 % and 0.35%, respectively. The analysis of the obtained results shows that a non-uniform 120x120 grid and the time step, *dt*=0.1 s, were found sufficient to give accurate results. A fine grid size near solids was set to give more details for hydrodynamic behavior near interfaces. Other smalltime steps were used but, supply a drastic CPU time, without giving appreciable accuracy in numerical results.

Table 2: Sensitivity of the results for varying grid (a) and time step (b). t=7200 s, Φ=1%

MxN	***F***	***Deviation (%)***	T_{max}	***Deviation (%)***
(a)				
80x80	0.231		59.1	
100x100	0.238	2.94	58.5	1.03
120x120	0.240	0.83	58.0	0.86
140x140	0.241	0.41	57.9	0.17

Time step, dt	***f***	***Deviation (%)***	T_{max}	***Deviation (%)***
(b)				
5 s	0.215		59.8	
1 s	0.235	8.51	58.6	2.05
0.1 s	0.240	2.08	58.0	1.03
0.05 s	0.242	0.83	57.8	0.35

2.6 Validation

The computer program was used for validation against experimental data obtained by Zivkovic and Fujii (2001). The work conducted by Zivkovic and Fujii (2001) consists of an experimental study of the melting of PCM $CaCl_2.6H_2O$, T_m=28°C, k=0.145 W/mK, ΔH_f =148.5 kJ/kg, ρ =981 kg/m^3, as nano phase change material with 2% Copper nanoparticles in an insulated 10 cm x 10 cm rectangular enclosure. The walls are made with 7.5 mm Plexiglas. Lateral sides of the rectangular container are well insulated and heat transfer occurs only from bellow by isothermal wall at T=30°C. The model was implemented by developing a personal computer code. The developed computer program was adjusted to reproduce experimental conditions, and the numerical predictions have been, next, compared to experimental data. Figure 2 displays the comparison between the numerical predicted and measured temperatures and temperatures obtained by Zivkovic and Fujii (2001). As shown in Figure 2, the temperature of centre of the container increases until reaches the melting point. Then the PCM absorb energy to change phase from solid to liquid in a constant temperature, then, the temperature will increase. Analysis of such figure shows a satisfactory agreement between the measured and calculated temperatures. The maximum deviation is found less than, 1%. The slightly difference in the temperature history appears when heat sources reach the plateau region (quasi steady state). It is due, at prior, to the surrounding heat lost that occurred during experimental tests.

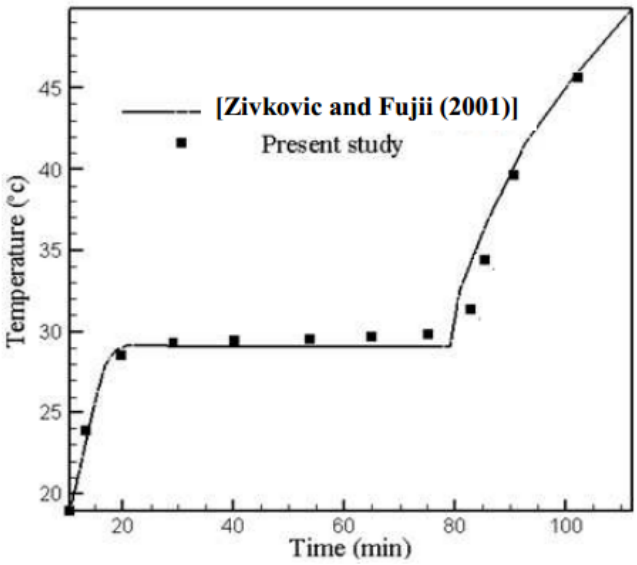

Figure 2: Comparison of numerical and experimental temperatures at the centre of the rectangular cavity.

3 Results and discussion

To ovoid the overheating of the heat source, numerical simulations were conducted during the limiting time t_{cr} required to reach limit temperature, T_{cr}. In this study, the effects of copper nanoparticles fraction, Φ, is examined. Numerical investigations were performed using the Table 3 data.

Table 3: Physical properties [Eastman, Choi, Thompson et al. (1997); Tummala (2001)]

Heat source (Alumina Ceramics)	***Conducting Plate (Alumina substrate)***	***Nanoparticles (CuO-Copper)***	***PCM (n-eicosane)***
ρ_c = 3260 kg/m^3	ρ_s = *1188 kg/m^3*	ρ_p = *8933 kg/m^3*	β = *8.5 10^{-4} K^{-1}*
$c_{p,c}$ = *740 J/kg K*	$c_{p,s}$ = *1445 J/kg K*	$c_{p,p}$ = *385 J/kg K*	ΔH_f = *2.47x10^5 J/kg*
k_c=*170 W/mK*	k_s=*0.193 W/mK*	k_p=*400 W/m K*	T_m=*47°C*
T_{cr}=*80 °C*		d_p=*60 nm*	$c_{p,m}$=*2460 J/kg K*
			k_m=*0.1505 W/mK²*
			ρ_m= *769 kg/m^3*
			μ_m= *4.15x10^{-3} kg/m s*

Figure 3 shows the time wise evolution of maximum heat source temperature, T_{max}, and liquid fraction, f, for various nanoparticles volumetric fractions, Φ=0%, 0.5%, 1%, 2% and 3%. Analysis of such figure shows that, heat source temperature, vary within 3 stages whatever the nanoparticles fraction is. At the first stage, heated source primes the melting

of a thin layer of PCM around the heat source. Temperature difference between heat source faces and the melting front is still weak that heat transfer occurs essentially by heat conduction. Isotherms are parallels to these surfaces. With time progress, heat source evacuates more energy in vicinity PCM and the maximum temperature rises rapidly due to the weak value of thermal conductivity of base PCM, (k_m=0.1505 W/m K, Φ=0). Note that, during the first stage of melting process, heat source maximum temperature rises rapidly to 67°C for ordinary PCM but increases only to 56°C for PCM with 3% of copper nanoparticles. As time elapses, the liquid cavity enlarges as can be seen at Figure 4a, and the driven temperature between the melting front (moving cold wall) and the bottom hot wall increases and create the liquid motion within molten phase. Hot and light liquid rises over the heat source and flays along the cold melting front, releases heat, and becomes cooled heavier, descends and turns over to the bottom wall and absorbs more heat from heat source. The heat transfer turns into natural convection, see Figure 5 below. The maximum temperature decreases sharply from 67°C to 63°C for ordinary PCM and from 56°C to 54°C for PCM with 3% copper nanoparticles. A pseudo steady state regime takes place. During the plateau region, horizontal segment of T curves, heat source maximum temperature is kept even constant. All energy generated by heat source is absorbed by the melting front as latent heat, and sensible heating disappears. As a result, the mean PCM temperature stays even constant. The melting front absorbs an important amount of the energy evacuated by heat source converted to latent heat of fusion. Liquid fraction increases quickly with time and nanoparticles concentration, as can be seen from f curves in Figure 3. The melting front (the cold wall) goes far from heat source. During the plateau period, heat source is efficiency cooled and works safely a long period without using any forced convection fans.

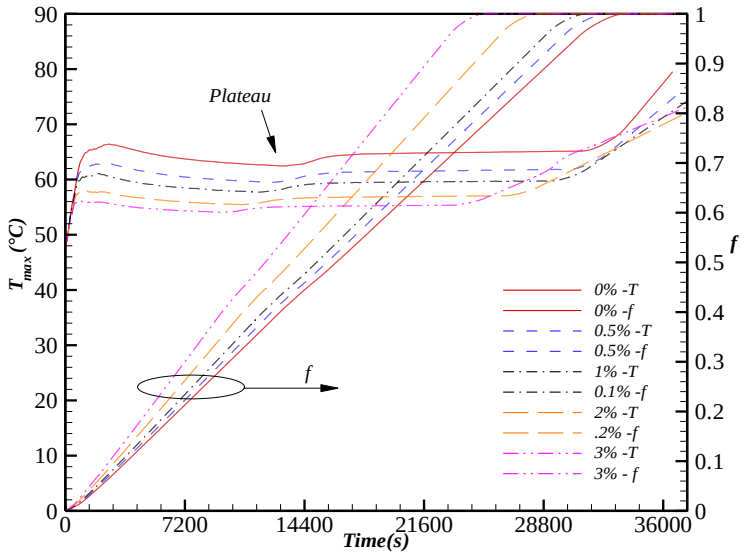

Figure 3: Maximum heat source temperature T_{max} and liquid fraction f for various nanoparticles fractions Φ.

Also, Figure 3 shows that the plateau period length decreases clearly with nanoparticule

fraction. In fact, heat source works safely during, $t_{plateau}$=8 h 45 min for the base PCM and, $t_{plateau}$=6 h 40 min for PCM with 3% nanoparticles. When adding more nanoparticles to base PCM, heat conduction is adorned, Eq. (6), and heat source evacuates it energy easily to phase change materiel, leading to fast PCM fusion. However, the early melting of nano PCM gives a situation of generating heat source without heat sink (absence of cold boundary). The last stage of the melting process takes place when heat source temperature re-increases. In fact, thermal resistance of the liquid cavity rises and liquid phase near heat source overheat and provokes a dramatic increase in heat source temperature which rises rapidly to critical temperature, T_{cr}, depending on nanoparticles fraction. During the third stage the device must stops to ovoid the damaging of heat source. It is worthy to notice that, depending to the electronic component (heat source) working conditions and sensitivity, there is a duality between working with lowest temperature during a small plateau period for more concentrated nano PCM or with even high temperature during lager plateau period for low particles fraction as can be seen in Figure 3.

Figure 4 and Figure 5 illustrate the computed isotherms and velocity field at different melting times for two volumetric fractions of copper nanoparticles dispersed in phase change material, heated from bellow using the protruding heat source. Analysis of Figure 4 shows that in the beginning of the melting process, conduction is the initial heat transfer mechanism. During this early stage, buoyancy cannot overcome the resistance imposed by the viscose forces. The cold fluid is above the warm one. The thermally unstable situation is broken when the thickness of the liquid layer increases and advection takes place in the liquid phase. Then, Rayleigh-Bénard flow pattern is observed during the progress of the melting. A complex structure of the fluid dynamics appears and characterized by a bi-cellular flow patterns, Figure 5 shows two convective cells locate above the bottom hot wall (conducting plate and heat source). The rotation of the Rayleigh-Bénard cells is stable and is clockwise and counter-clockwise for the left and the right roll respectively. Convective flow strengthens and remains bi-cellular. Natural convection current enters extends and continue in the rest of the melting process, resulting in faster melting rate in fact liquid fraction increase linearly, as shown in Figure 3 above, during the plateau period. As the melting front progresses, the liquid domain extends and the two cells grow in size but never combine, Figure 5. The isotherms, at the beginning of the melting process, were parallel to the hot bottom boundary of the enclosure due to a dominating role of heat conduction. As time elapses, the effect of convection is seen as a departure of the isotherms from being parallel to the hot wall, Figure 4, t=10 min. During the plateau stage, t=120 min, the mechanism of heat transfer is shifted to natural convection, and a wall jet rises above heat source and the panache structure of isotherms appears due to the counter-rotating convective cells. The deformation of the isotherms and then the curvature of the melting interface become more accentuated.

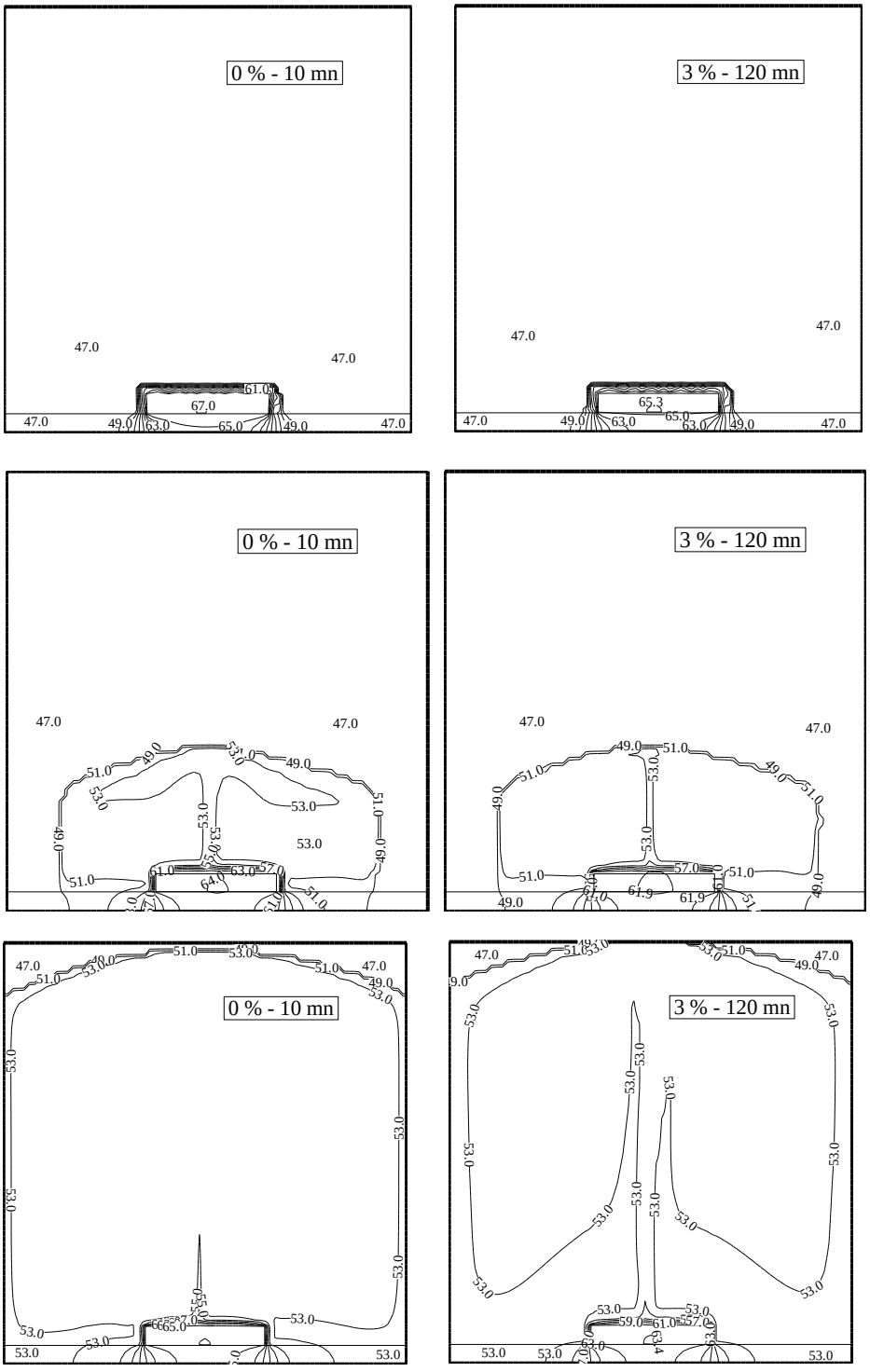

Figure 4: Isotherms evolution for Φ=3% and Φ=0%.

Comparison of isotherms, Figure 4, reveals that the deformation due to natural convection effect is less for Φ=3%, Nanoparticles increase the dynamic viscosity and reduce natural convection intensity which develops in the molten PCM. As a result, temperature of the liquid zone becomes more homogeneous than its counterpart with 0% of nanoparticles where isotherms are clearly disturbed at t=120 min. Figure 4 exhibits that for nanoparticles fraction Φ=3%, the initial conductive regime mixes rapidly with a light natural convection which develops in the liquid PCM. The liquid cavity grows rapidly due to the improvement of thermal conductivity, and heat source temperature stabilizes quickly at secured level and the molten cavity is almost isothermal, unlike the base fluid, Φ=0%, where heat source is more heated and isotherms are distorted due to the strong convective current, Figure 5.

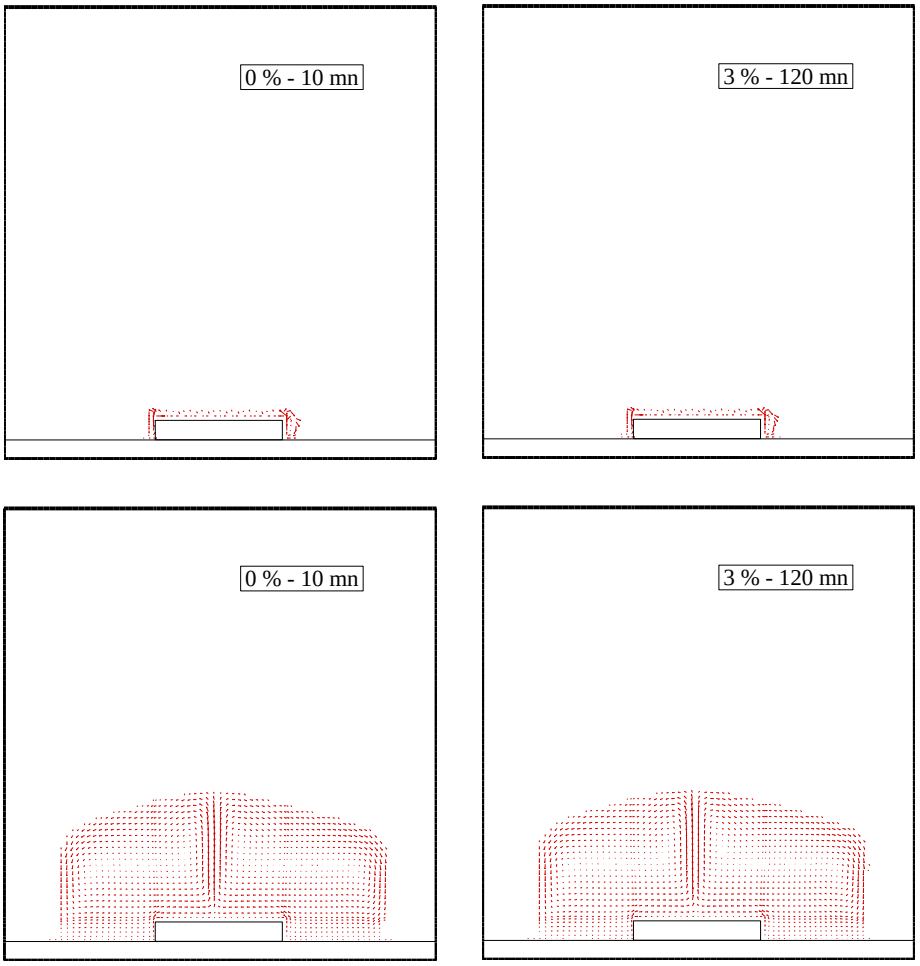

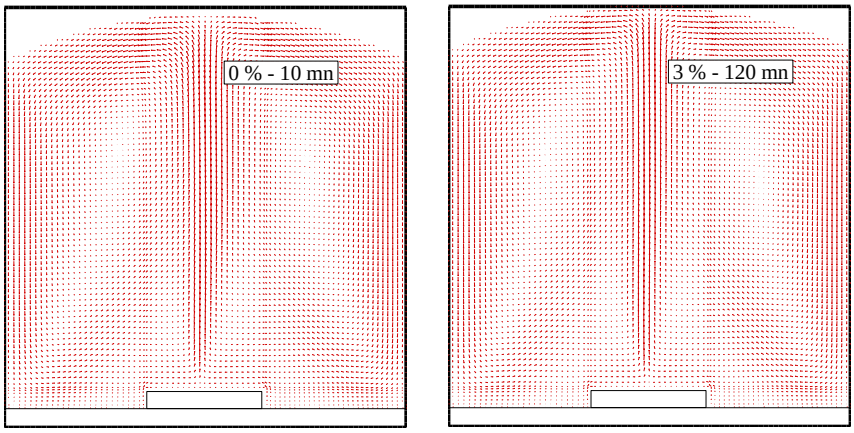

Figure 5: Velocity field evolution for Φ=3% and Φ=0%.

Figure 6 shows the effect of the nanoparticles fraction, Φ, on the temperature distribution within the plate, at different melting periods. It can be seen that with the increase of the nanoparticles fraction, Φ, the plate and heat sources are well cooled. When Φ raises, heat spreads profoundly along the plate and consequently to the PCM. As a result, heat transfer through the plate and heat source faces is enhanced, which allows to a reduction of heat sources temperatures. It can also be seen that increasing in the nanoparticles fraction, Φ, leads to a reduction in the maximum temperature difference, ΔT_{plate}, that can be found in the plate. This difference is equal, during the quasi steady state period, to ΔT_{plate}= 14.7°C and ΔT_{plate}=16.9°C for, Φ=3% and, Φ=0%, respectively.

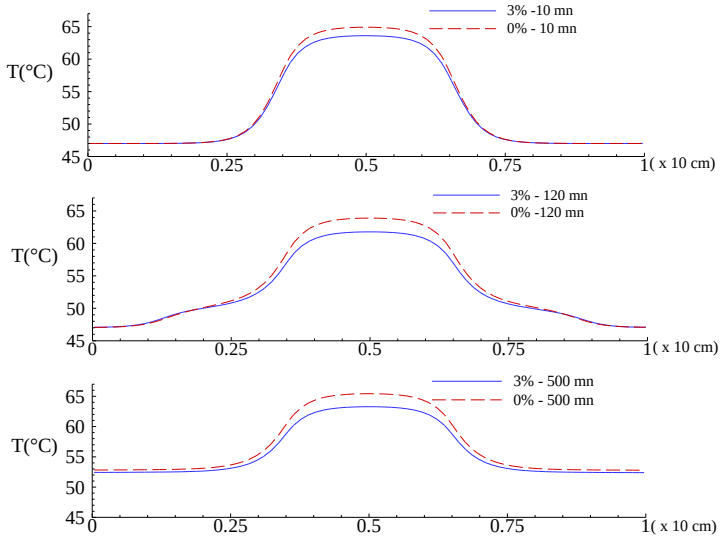

Figure 6: Substrate (plate) temperature profile dependency on the nanoparticles fraction, Φ, at different melting periods (y= e_s/2)

Figure 7 represents the maximum heat source temperature during the plateau stage T_{work}

and the secured working time, $t_{plateau}$, as functions of nanoparticle fraction. Analysis of Figure 6 substantiates the doubt concerning the effective enhancement in the PCM cooling performance due to dispersing the nanoparticles, relative to the simple PCM. The effective thermal conductivity of the nano PCM improvement could be outweighed by the rise in the dynamic viscosity. Also, heat sinking capability, for a given PCM enclosure size, depends closely to the particles volumetric fractions. The maximum amount of energy that can be dissipated in PCM decreases with the increase of the added particles. That reduces the volume occupied by the base PCM. Also, the increase in dynamic viscosity will extinguish the role of natural convection heat transfer with the excess of nanoparticles across the melted region. And, as mentioned above, the damping convection current creates a near isothermal homogeneous liquid. Therefore, there is an optimal volumetric fraction of nanoparticles, to be added, which exhibits lower working temperature with adequate working time.

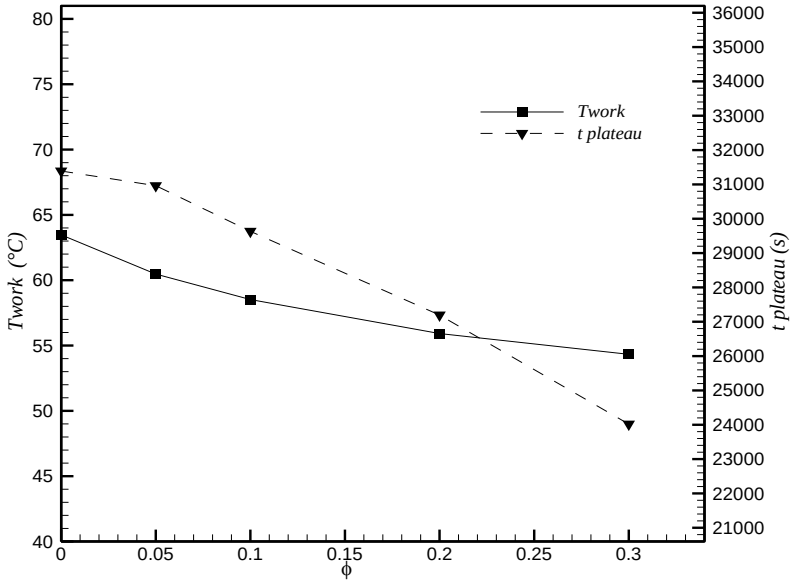

Figure 7: Maximum heat source temperature, T_{work}, and secured working time, $t_{plateau}$, as functions of nanoparticle fraction, Φ

Based on Figure 7 data, the working temperature T_{work} and the secured working time $t_{plateau}$ are correlated to the nanoparticle fraction by equation, (Eq. 14), with accuracy 8% and, (Eq. 15), with accuracy 5%, respectively.

$$T_{work}=-29.2\,\Phi + 62.3\ (°C),\quad 0< \Phi<0.03 \tag{14}$$

$$t_{plateau}=-25173\Phi + 31912\ (s),\quad 0< \Phi<0.03 \tag{15}$$

4 Conclusion

In this study, the effect of copper nanoparticles fraction on cooling capability of protruding heat source embedded in rectangular cavity, filled with PCM is numerically investigated. In order to enhance the heat source working time and working temperature low percentage

of nanoparticles were dispersed in the PCM enclosure. The thermal resistance is reduced due to the important value of the thermal conductivity of nanoparticles. In contrast, the dynamic viscosity also increases, and reduces the natural convection strength. Results reveal that the increment of volume fraction of nanoparticles causes more stability of heat source temperature during the quasi steady state regime period. An increase in nanoparticles from, 0% to 3%, leads to improved heat spreading within the liquid phase, as is indicated by enhancement in working temperature that reduced from 67°C to 55°C. However, the increase in particles fraction shifts convection currents, reducing the time it takes the PCM to melt completely and decrease the secured working time because the fast melting of solid PCM induces an early superheating of heat source and reduces its working time.

References

Afrouzi, H. H.; Farhadi, M. (2013): Mixed convection heat transfer in a lid driven enclosure filled by nanofluid. *Iranica Journal of Energy and Environment*, vol. 4, pp. 376-384.

Bianco, V.; Manca, O.; Nardini, S.; Vafai, K. (2015): *Heat Transfer Enhancement with Nanofluids*, CRC Press.

Bouchoucha, A.; Bessaih, R. (2015): Natural convection in a square cavity filled with nanofluids. *Fluid Dynamics and Material Processing*, vol. 11, no. 3, pp. 279-300.

Cabeza, L. F.; Castellón, C.; Nogués, M. (2007): Use of microencapsulated PCM in concrete walls for energy savings. *Energy and Buildings*, vol. 39, pp. 113-119.

Eastman, J. A.; Choi, S.U.S.; Li, S.; Thompson, L. J.; Lee, S. (1997): Enhanced thermal conductivity through the development of nanofluids, in: S. Komarneni, J.C. Parker, H.J. Wollenberger (Eds.). *Nanophase and Nanocomposite Materials II*, MRS, Pittsburg, PA, pp. 3-11.

Faraji, M.; El, Q. H. (2009): Passive cooling of protruding electronic components by latent heat of fusion storage. ASME. *Journal of Electronic Packaging*, vol. 131, no. 2, pp. 68-77.

Gong, Z. X.; Devahastin, S.; Mujumdar, A. S. (1999): Enhanced heat transfer in free convection-dominated melting in a rectangular cavity with an isothermal vertical wall. *Applied Thermal Engineering*, vol. 19, pp. 1237-1251.

Hao, Y. L.; Tao, Y. X. A (2004): Numerical model for phase-change suspension flow in microchannels. *Numerical Heat Transfer, Part A*, vol. 46, pp. 55-77.

Khodadadi, J. M.; Hosseinizadeh, S. F. (2007): Nanoparticle-enhanced phase change materials (NEPCM) with great potential for improved thermal energy storage. *International Communications in Heat and Mass Transfer*, vol. 34, no. 5, pp. 534-543.

Maxwell, J. A. (1904): *Treatise on Electricity and Magnetism*. Oxford University Press, Cambridge, UK.

Patankar, S. V. (1980): *Numerical Heat Transfer and Fluid Flow*. Hemisphere, Washington, D.C.

Saha, S. K.; Srinivasan, K.; Dutta, P. (2008): Studies on Optimum Distribution of Fins

in Heat Sinks Filled with Phase Change Materials. *Journal of Heat Transfer*, vol. 130, no. 3, pp. 171-181.

Sanusi, O.; Warzoha, R.; Fleischer, A. S. (2011): Energy storage and solidification of paraffin phase change material embedded with graphite nanofibers. *International Journal of Heat and Mass Transfer*, vol. 54, no. 19-20, pp. 4429-4436.

Tong, X.; Khan, J.; Amin, M. R (1996): Enhancement of Heat Transfer by Inserting a Metal Matrix into a Phase Change Material. *Numerical Heat Transfer, Part A*, vol. 30, no. 2, pp. 125-141.

Tummala, R. R. (2001): *Fundamentals of Micro systems Packaging*. McGraw Hill.

Vajjha, R. S.; Das, D. K.; Namburu, P. K. (2010): Numerical study of fluid dynamic and heat transfer performance of Al2O3 and CuO nanofluids in the flat tubes of a radiator. *International Journal of Heat Fluid Flow*, vol. 31, pp. 613-621.

Valan, A.; Mujumdar, A. S. (2012): Numerical study on melting of paraffin wax with Al_2O_3 in a square enclosure. *International Communication in Heat and Mass Transfer*, vol. 39, pp. 8-16.

Voller, V. R.; Cross, M.; Markatos, N. C. (1987): An enthalpy method for convection/diffusion phase change. International Journal for Numerical Methods in Engineering, vol. 24, no. 1, pp. 271-284.

Wu, S.; Zhu, D.; Zhang, X.; Huang, J. (2010): Preparation and melting/freezing characteristics of Cu/paraffin nanofluid as phase change material (PCM). *Energy and Fuels*, vol. 24, no. 3, pp. 1894-1898.

Weinstein, R.; Kopec, T.; Fleischer, A.; Addio, E.; Bessel, C. (2008): The experimental exploration of embedding phase change materials with graphite nanofibers for the thermal management of electronics. *Journal of Heat Transfer*, vol. 130, pp. 042405-1-042405-8.

Zivkovic, B.; Fujii, I. (2001): An analysis of isothermal phase change of phase change material within rectangular and cylindrical containers. *Solar energy*, vol. 70, pp. 51-61.